New Journal of Physics
The open-access journal for physics

Ordering and self-diffusion in FePt alloy film

M Gupta[1,6], A Gupta[2], J Stahn[3] and T Gutberlet[4,5]

[1] UGC–DAE Consortium for Scientific Research, BARC, Mumbai 400 085, India
[2] UGC–DAE Consortium for Scientific Research, Khandwa Road, Indore 452 017, India
[3] Laboratory for Neutron Scattering, ETH Zürich and Paul Scherrer Institut, 5232 Villigen PSI, Switzerland
[4] Laboratory for Neutron Scattering, ETH Zürich and Paul Scherrer Institut, 5232 Villigen PSI, Switzerland
E-mail: mgupta@csr.ernet.in

New Journal of Physics **10** (2008) 053031 (8pp)
Received 18 February 2008
Published 22 May 2008
Online at http://www.njp.org/
doi:10.1088/1367-2630/10/5/053031

Abstract. Neutrons have different scattering cross-sections for the isotopes of an element. Also, they interact with the un-paired electrons in a magnetic sample due to their magnetic moment. Neutron reflectivity or reflectometry is a technique which measures the depth profile of a sample. Using polarized neutrons, both self-diffusion and magnetism can be probed in a unique way. In the present work, polarized neutron reflectometry measurements were performed in [FePt/^{57}FePt] multilayers across the structural ordering temperature of this sample. It was found that the structural ordering in this system is concurrent with a sudden increase in Fe diffusivity and a sudden drop in the value of the magnetic moment.

[5] Present address: Forschungszentrum Jülich GmbH, Jülich Centre for Neutron Science at FRM II, 85747 Garching, Germany.
[6] Author to whom any correspondence should be addressed.

Contents

1. Introduction

Recently, intermetallic compounds such as FePt have emerged as potential candidates for high-density magnetic recording media and high-energy permanent magnets due to their large magneto-crystalline anisotropy. The FePt system exhibits a canonical phase diagram based on fcc structures with three-ordered phases Fe_3Pt (γ_1, $L1_2$), FePt (γ_2, $L1_0$) and $FePt_3$ (γ_3, $L1_2$). In particular, the $L1_0$ phase offers next generation data storage devices in the range of 1 $Tbin^{-2}$ which is three orders of magnitude larger than present day devices [1, 2]. Many attempts have been made to prepare FePt ordered phases using co-sputtering, and the structural and magnetic properties have been investigated. It was found that the ordering in this system starts in the temperature range of 600–800 K [3] and above 1500 K a order–disorder transition takes place [4].

It might be surprising to note that very little diffusion data are available on this system except for high-temperature radio-tracer data in the disordered state. Also, it is not known how diffusivity would change when a transition is taking place. This is partly due to the fact that around the ordering temperature, the diffusion is much smaller than the resolution of the techniques used for the measurements (e.g. secondary ion mass spectroscopy, radioactive tracer method etc). In a recent work, Rennhofer *et al* [4] studied Fe self-diffusion in $L1_0$-ordered FePt thin films using nuclear resonance reflectometry. It may be noted that reflectometry or grazing incidence reflection offer a depth resolution down to Aangstrom level [5]. Both x-ray reflectivity (XRR) and neutron reflectivity (NR) techniques when applied to study thin films and multilayers give quantitative information on the composition and structure of the sample in a non-destructive way. In particular, neutrons have certain advantages when compared to x-rays: (i) neutrons have comparable sensitivity to light and heavy elements and they are even sensitive to isotopes, allowing for elegant experiments with contrast variation and (ii) they are sensitive to magnetism, i.e. the neutron scattering length (a measure for the nuclear or magnetic potential seen by the neutron) is modified in the presence of un-paired electrons.

Using polarized neutron reflectivity (PNR) information on both, the structure and the magnetism of a sample can be probed in a unique way. The neutron scattering lengths for natural Fe and ^{57}Fe are 9.45 and 2.3 fm, respectively. Therefore, a sample of the FePt alloy with a periodic setup-like modulation of the ^{57}Fe isotope concentration would allow for studying Fe self-diffusion in this alloy. At the same time, reflectivity measurements using polarized neutrons would yield information on the magnetism of this alloy.

2. Experimental

FePt alloy thin films were deposited using ion beam sputtering. The ion beam source used to produce Ar^+ ions was a Kaufman-type hot cathode ion gun installed in a vacuum chamber at

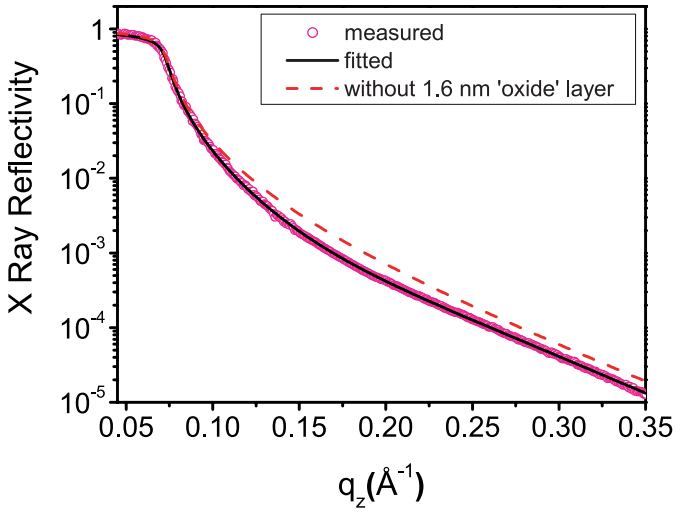

Figure 1. XRR pattern of the Si/[FePt 9 nm/^{57}FePt 5 nm]$_{10}$ sample. Due to similar scattering cross-sections for Fe and ^{57}Fe, the pattern does not show any features. The dashed line shows a pattern in the absence of the 1.6 nm 'oxide' layer.

an angle of 45°. The Ar^+ ions were allowed to fall alternatively on [Fe + Pt] and [^{57}Fe + Pt] composite targets to deposit a multilayer structure [FePt 9 nm/^{57}FePt 5 nm]$_{10}$ on a Si(100) substrate. The pressure during the deposition of the films was of the order of 10^{-3} mbar while the pressure obtained before inserting Ar gas in the chamber was about 10^{-6} mbar. More details about sample preparation are given in [6, 7]. The composition of the FePt alloy was determined using EDAX to be $Fe_{0.5}Pt_{0.5}$. The crystal structure of the samples was determined using x-ray diffraction (XRD). The thickness and the scattering contrast between the layers in the multilayer were measured using XRR and unpolarized NR. Fe diffusion and magnetic induction in the samples were obtained using PNR. X-ray measurements (diffraction and reflectivity) were performed with a laboratory source using Cu–Kα x-rays of wavelength 1.54 Å. Both unpolarized NR and PNR measurements were performed at the reflectometer AMOR at the Swiss spallation neutron source (SINQ), at Paul Scherrer Institute, Switzerland [8]. The reflectivity pattern was measured using different angular settings in the time-of-flight (TOF) mode. High-temperature annealing of the films was performed using a vacuum furnace. The typical pressure during annealing was of the order of 10^{-6} mbar.

3. Results and discussions

The thickness and the layer structure of the deposited multilayer were determined using XRR and NR. Since there is no contrast between FePt and ^{57}FePt for x-rays, it is expected that the XRR of this sample would lead to a pattern analogous to a thin film. Figure 1 shows the XRR pattern of this sample. Detailed fitting of these data reveals that there is a thin layer of about 1.6 nm at the surface of the sample, which may have formed due to oxidation of the sample when exposed to the atmosphere. In the fitting model if we exclude this layer the pattern would be given by the dashed line as shown in figure 1.

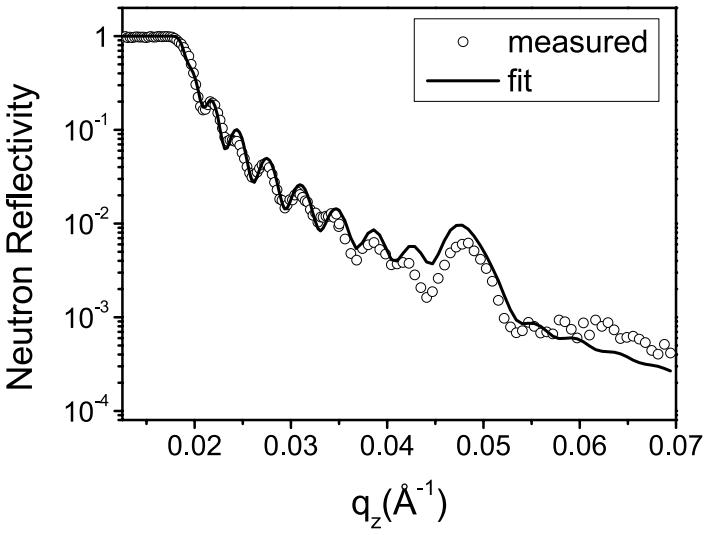

Figure 2. NR pattern of the Si/[FePt 9 nm/^{57}FePt 5 nm]$_{10}$ sample. Due to different scattering cross-sections for Fe and ^{57}Fe, a multilayer Bragg peak appears in the pattern. The oscillations correspond to the total thickness of the multilayer.

It is expected that the NR of this sample gives rise to a Bragg peak due to the periodicity of the ^{57}Fe/Fe isotope concentration. Figure 2 shows the NR pattern of the Si/[FePt 9 nm/^{57}FePt 5 nm]$_{10}$ sample. One can see a well-defined Bragg peak appearing in the neutron data while with x-rays no such structure is visible. This confirms that there is no chemical contrast between the FePt and the ^{57}FePt layers and only the isotope contrast leads to the Bragg peak in the NR data. From the NR data shown in figure 2, the following information could be obtained: (i) the oscillations corresponds to the total thickness of the sample. (ii) The position of the Bragg corresponds to the period ($\ell \equiv$ FePt +^{57} FePt) of the bilayer. With a single Bragg peak the individual layer thickness could not be obtained. However, in our case since both the layers are chemically homogeneous the rate of deposition in both the cases would be similar, therefore with known deposition time, the individual layer thickness of FePt and ^{57}FePt layers could be quantified. The detailed fitting of the NR data gives the structure of the multilayers: Si/[FePt (9 nm)/^{57}FePt (4.9 nm)]$_{10}$ as shown in figure 3. The roughness of the interfaces is in the range of 1–2 nm. The fitting of the experimental data was performed using the program PARRAT32 [9].

The crystal structure of the films as-deposited and annealed at higher temperatures was determined using XRD. Figure 4 shows the XRD pattern obtained in the as-deposited state and after annealing the samples at different temperatures. Up to an annealing temperature of 573 K, the XRD pattern appears similar to that of as-deposited samples. In the as-deposited samples annealed up to 573 K diffraction peaks predominantly corresponding to Pt are seen. Though some reflections corresponding to Pt and FePt appear at similar angles, the superlattice reflection, unique to FePt phase, could not be seen in the as-deposited sample and samples annealed up to 573 K. However, after annealing at 673 K, the peaks corresponding to the FePt phase starts to appear, indicating that ordering in this system starts at 673 K. The peaks appearing around 32.9°, 53° and 59° are superlattice peaks corresponding to $L1_0$-ordered

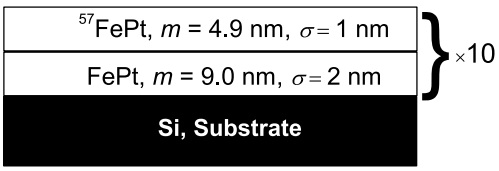

Figure 3. Representation of the fitted parameters obtained from the NR pattern shown in figure 2. m stands for the thickness of a layer and σ for the roughness of the (upper) interfaces.

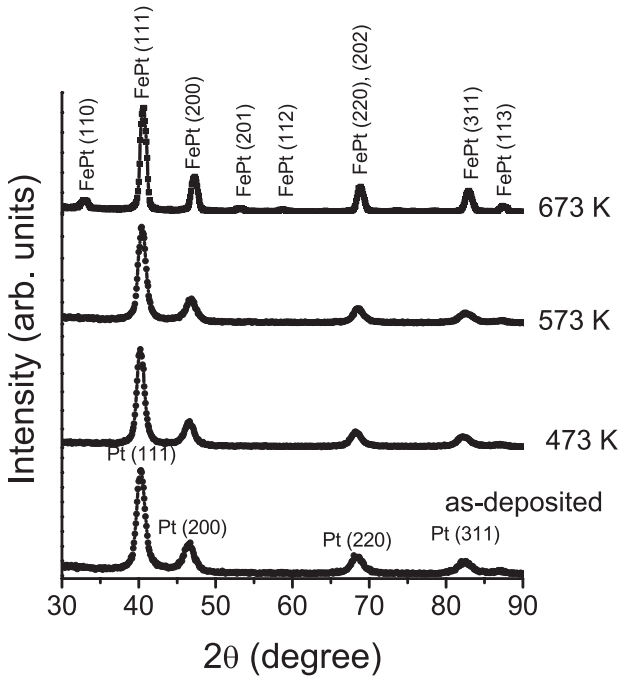

Figure 4. XRD pattern of the Si/[FePt 9 nm/^{57}FePt 5 nm]$_{10}$ sample in the as-deposited state and after annealing at different temperatures. The ordering in this sample starts after annealing above 573 K.

phase. [10]. The details of such structural evolutions were also studied by us in an earlier work on Fe/Pt multilayers [7].

In order to calculate the diffusion and magnetic moment of the samples, PNR measurements were performed. A magnetic field of 1 T was applied parallel to the surface of the samples, which is sufficient to saturate the sample magnetically. As the diffusion across the interfaces in the multilayer takes place the intensity of the Bragg peak in the PNR pattern decreases. This decrease in intensity is a measure of diffusion which is quantified by [11, 12]:

$$I(t) = I(0)\ \exp\left(-\frac{8\pi^2 n^2 D}{\ell^2}\, t\right), \tag{1}$$

where $I(0)$ is the intensity of the nth-order Bragg peak at time $t = 0$ (before annealing), D is the diffusivity, and ℓ is the bilayer periodicity. In order to calculate the diffusion, the multilayer

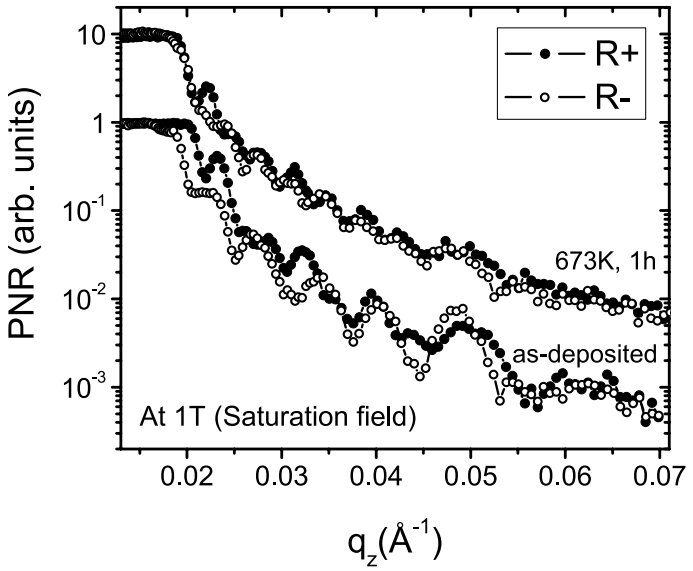

Figure 5. PNR pattern of the sample Si/[FePt 9 nm/^{57}FePt 5 nm]$_{10}$ in the as-deposited state and after annealing at 673 K for 1 h. The PNR measurements were carried out using a TOF reflectometer (AMOR, SINQ, PSI). The solid circles represent data taken with a neutron beam whose polarization and direction of magnetic field are parallel and open circles represent the cases when they are antiparallel.

sample was annealed at 373, 473, 573 and 673 K. A typical decay of the Bragg peak intensity after annealing at 673 K for 1 h is shown in figure 5. As can be seen, the intensity at the Bragg peak almost disappears after annealing at 673 K. However, annealing at lower temperatures, e.g. between 373 and 573 K, results in a small decrease in the intensity at the Bragg peak. Equation (1) gives the value of the diffusion coefficient, D at each temperature. A plot of D against the inverse of the temperature yields the relation between diffusion and temperature which is given by

$$D = D_0 \exp\left(-\frac{E}{k_B T}\right), \tag{2}$$

where D_0 is the pre-exponential factor, E the activation energy and k_B Boltzmann's constant. The obtained diffusivities are plotted in figure 6 as a function of $1/T$. As can be seen, up to a temperature of 573 K, there is a slight increase in the diffusivity with the increase in temperature. However, at a temperature of 673 K, where ordering starts, a sudden increase in the diffusivity can be observed. This suggests that as the structural ordering for the $L1_0$ phase starts, Fe diffuses rapidly across the interfaces.

PNR is a technique which is able to yield the absolute value of a magnetic moment per atom in a magnetic thin film with high accuracy [13]. In contrast to the bulk magnetization magnetometer techniques, e.g. dc extraction, VSM, or SQUID, no correction due to the magnetic signal from the substrate has to be applied in PNR. Further, the sample dimensions and mass do not play a crucial role in the determination of the magnetic moment. During the experiment, polarized neutrons with spin parallel or anti-parallel (also termed as spin + / up, or spin − / down) to the direction of magnetization on the sample are reflected off the surface

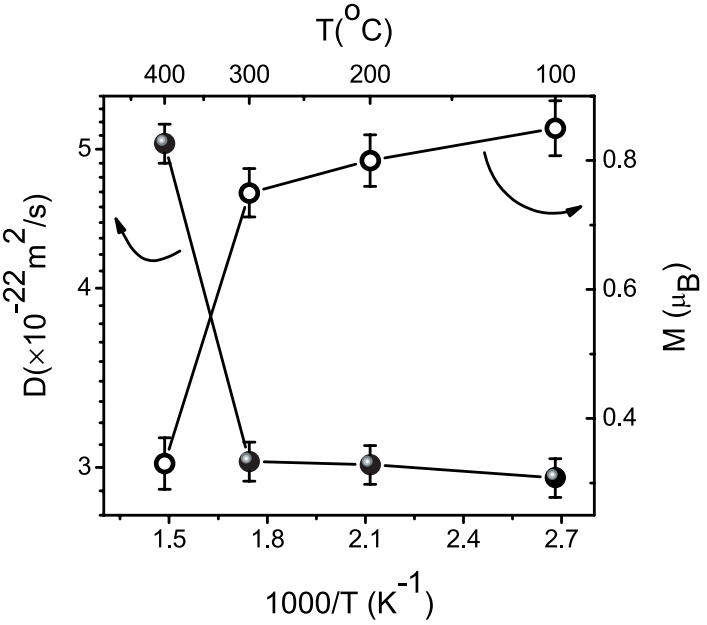

Figure 6. Calculated values of diffusivity and magnetic moment for the sample Si/[FePt 9 nm/^{57}FePt 5 nm]$_{10}$. The values of diffusivity were obtained using equations (1) and (2) while the value of the magnetic moments were obtained using equation (3).

of a sample at grazing incidence. The measurements were performed with an applied field of 1 T, which is sufficient to reach the saturation magnetization in all the layered samples. The measurements were carried out in the TOF mode at a fixed angle of incidence. The TOF–PNR has an advantage as during the measurement of spin-up and -down reflectivities, only the polarization of the incoming beam is changed by switching the direction of the applied field at the polarizing supermirror. No movement of the sample is required. The potential energy of a neutron in the ith region of the sample is given by [14, 15]

$$V_i = \frac{2\pi\hbar^2}{m_n}\rho_i b_i + \mu_n \cdot \mathbf{B}_i, \tag{3}$$

where m_n, ρ_i, b_i, μ_n and $\mathbf{B}_i$ are the mass of a neutron, the atomic density, the coherent scattering length, the neutron magnetic moment and the magnetic induction. The spin-dependence enters via the sign of the vectorproduct $\mu_n \cdot \mathbf{B}_i$.

Figure 5 shows spin-up and -down reflectivities in the as-deposited state and after annealing at 673 K. It can be seen that the separation between spin-up and -down reflectivities decreases (near the critical edge) indicating a decrease in the magnetic induction in the sample. The magnetic moment per Fe atom after each stage of annealing was calculated and is plotted in figure 6. Up to a temperature of 573 K, where the structure of the sample does not change, the magnetic moment shows a marginal decrease with an increase in the temperature. However, as the ordering in the system starts, there is a sudden drop in the value of the magnetic moment. This indicates that as the ordering in the FePt system starts, both diffusion and magnetism show a sharp change in their respective values. A decrease in the magnetic moment could be understood due to the formation of an ordered phase. Whereas a sharp increase in diffusivity suggests that the formation of the alloy is due to enhanced Fe diffusion. This indicates that $L1_0$

ordering in the FePt system is driven kinetically. However, in order to calculate the activation energy during the formation of the ordered phase more measurements will be required in the temperature range of 573–673 K with smaller steps in annealing temperature.

Acknowledgments

We acknowledge the help received from Mr M Horisberger and Mr S Potdar in sample preparation. This work is based on experiments performed at the Swiss spallation neutron source SINQ, Paul Scherrer Institut, Villigen, Switzerland.

References

[1] Tang Y J, AuBuchon J F, Chen L H, Jin S, Kin J W, Kim Y H and Yoon C S 2006 *J. Appl. Phys.* **99** 08G909
[2] Klemmer T, Hoydick D, Okumura H, Zhang B and Soffa W A 1995 *Scr. Metall. Mater.* **33** 1793
[3] Ito H, Kusunoki T, Saito H and Ishio S 2004 *J. Magn. Magn. Mater.* **272–276** 2180
[4] Rennhofer M *et al* 2006 *Phys. Rev.* B **74** 104301
[5] Gupta M, Gupta A, Stahn J, Horisberger M, Gutberlet T and Allenspach P 2005 *Phys. Rev.* B **70** 184206
[6] Gupta M, Gupta A, Phase D M, Chaudhari S M and Dasannacharya B A 2003 *Appl. Surf. Sci.* **205** 309
[7] Kavita S, Reddy V R, Gupta A and Gupta M 2005 *Hyperfine Interact.* **160** 157
[8] Gupta M, Gutberlet T, Stahn J, Keller P and Clemens D 2004 *Pramana J. Phys.* **63** 57
[9] Braun C 1999 *PARRATT32 or the reflectometry tool* (*HMI, Berlin*) 1997 1999 Online at http://www.hmi.de/bensc/instrumentation/instrumente/v6/refl/parratt_en.htm
[10] Baia J, Yanga Z, Weia F, Matsumotob M and Morisakob A 2003 *J. Magn. Magn. Mater.* **257** 132
[11] Mizoguchi T and Murata M 1991 *Japan. J. Appl. Phys.* **30** 1818
[12] Schmidt H, Gupta M, Gutberlet T, Stahn J and Bruns M 2008 *Acta Metall.* **56** 464–70
[13] Blundell S J and Bland J A C 1992 *Phys. Rev.* B **46** 3391
[14] Gupta R and Gupta M 2005 *Phys. Rev.* B **72** 024202
[15] Hope S *et al* 1997 *Phys. Rev.* B **55** 11422